Biol. Cybern. 44, 157–165 (1982)

Biological Cybernetics

Multiplication Noise in the Human Visual System at Threshold 3. The Role of Non-Poisson Quantum Fluctuations*

Malvin Carl Teich[1], Paul R. Prucnal[1], Giovanni Vannucci[2], Michael E. Breton[3], and William J. McGill[4]

1 Department of Electrical Engineering, Columbia University, New York, NY, USA
2 Bell Laboratories, Holmdel, NJ, USA
3 Department of Visual Physiology, Wills Eye Hospital, Philadelphia, PA, USA
4 Department of Psychology, University of California at San Diego, La Jolla, CA, USA

Abstract. Several kinds of light used in vision experiments produce photon statistics that are distinctly non-Poisson. Representative examples are light from a cathode-ray tube and an image-intensifier device. For the class of vision experiments in which the photon statistics play an important role, excess fluctuations produced by such light sources can alter the observed results and obscure the visual mechanisms being studied. They must therefore be accounted for in a proper way. We use the results of a Hecht-Shlaer-Pirenne type experiment, carried out with modulated Poisson light, to illustrate the point. Sensitivity and modulation depth, as well as sensitivity and reliability, are shown to be traded against each other. Finally, we demonstrate that number-state light, which is comprised of photons of an ideal kind, provides the ultimate tool for extracting information about the intrinsic noise distribution in the visual system at threshold. The state of the art in producing such light is discussed.

1. Introduction

Vision experiments are conducted with many different kinds of light sources. These include incandescent filaments, lasers, light-emitting diodes (LEDs), and cathode-ray tubes. In some experiments, particularly those conducted at low light levels, the statistical character of the light source is a matter of some importance. The quintessential example is the experiment of Hecht et al. (1942). It is generally assumed in the vision literature, usually tacitly, that the photon statistics for all light sources are Poisson. For Poisson light, the ratio R of count variance $\langle(\Delta n)^2\rangle$ to count mean $\langle n\rangle$ is precisely unity.

* This work was carried out at Columbia University and was supported by the National Science Foundation and the National Institutes of Health

The purpose of this paper is threefold. First we wish to demonstrate that the photon statistics for some commonly used light sources are distinctly non-Poisson. A principal example is cathodoluminescence light (e.g., light from a cathode-ray screen such as an oscilloscope). Because of the generation mechanism, cathodoluminescence photons result from a multiplication or cascade of two Poisson processes, and are emitted in clusters. Thus R can be substantially greater than unity. Radiation of this character is sometimes called multiplied-Poisson light or shot-noise light (Teich and Saleh, 1981a).

Second, we point out that a Hecht-Shlaer-Pirenne (HSP) experiment conducted with multiplied-Poisson light or, indeed, with any kind of bunched light ($R>1$), will generate psychometric functions that differ in shape from those obtained with Poisson light. To illustrate the effect, we carried out a series of experiments with light that was purposely modified from its Poisson form by triangular intensity modulation. Our results show that the excess fluctuations associated with such light cannot be used constructively to provide information about the workings of the visual system, beyond that provided with Poisson light.

Third, we show that such additional information could be made available by carrying out an HSP-type experiment with a kind of ideal light called number-state light. The photons from such a source are spread perfectly evenly in time so that $R=0$. Though number-state light has not yet been generated in the laboratory, recent theoretical and experimental results in quantum electrodynamics show that it is possible to produce light for which $0<R<1$. Such light is called "anti-bunched", indicating that the emitted photons are less clustered than those for Poisson light.

In Part 1 of this set of papers (Teich et al., 1982), we dealt with Poisson quantum fluctuations and the minimum-detectable energy; in Part 2 (Prucnal and Teich, 1982), we used the normalizing transform and

0340-1200/82/0044/0157/$01.80

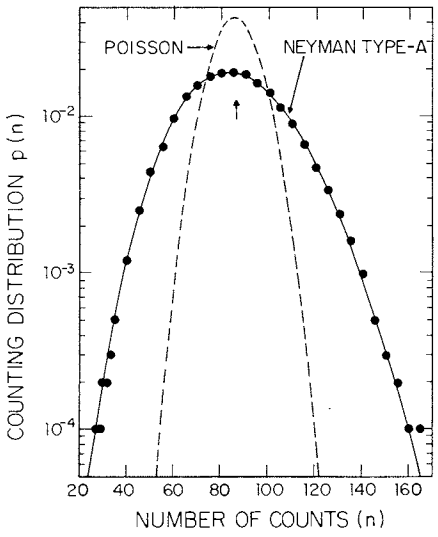

Fig. 1. Photon-counting distribution $p(n)$ vs number of photon counts n for radioluminescence light (solid dots). The solid curve represents the Neyman type-A counting distribution with the same values of count mean and variance. A Poisson distribution with the same mean is shown as the dashed curve. (After Teich and Saleh, 1981a)

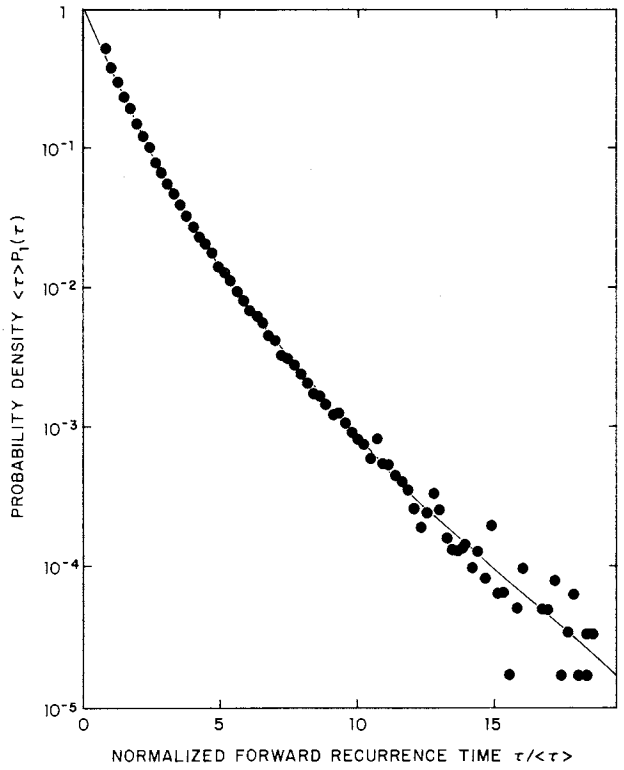

Fig. 2. Forward-recurrence-time probability density $\langle\tau\rangle P_1(\tau)$ vs time, for cathodoluminescence light (solid dots). The solid curve represents the theoretically expected result. Poisson light would obey an exponential density function, a straight line on this plot. (After Saleh and Teich, 1982a)

probit analysis to provide improved estimates of threshold parameters for Poisson light.

2. Statistical Properties of Multiplied-Poisson Light

We have recently carried out an extensive study of multiplied-Poisson light (Teich, 1981; Teich and Saleh, 1981a, b; Saleh and Teich, 1982a, b). Cathodoluminescence, the phenomenon responsible for the oscilloscope image, provides an example of how light with these statistical properties is generated. A primary beam of electrons, with Poisson arrival times, impinges on a phosphor. Each electron produces a Poisson number of photons, with the average number of photons per electron given by α'. The emission times are determined by the lifetime of the phosphor, τ'_p. If the detector counting time T' is $\gg\tau'_p$, and the quantum efficiency for detection is η', the resultant photon-counting distribution is describable by the Neyman Type-A (NTA) counting distribution, for which (Neyman, 1939; Teich, 1981; Teich and Saleh, 1982)

$$R=1+\eta'\alpha'>1\,. \tag{1}$$

Image-intensified light (van Meeteren, 1978) behaves similarly.

To demonstrate this, we provide two experimental results for luminescence light. In Fig. 1, the solid dots represent the observed photon-counting distribution $p(n)$ vs the number of photon counts n for radioluminescence photon registrations from the glass faceplate of a photomultiplier tube (Teich and Saleh, 1981a). The counting time ($T'=0.4$ ms) was chosen to be much greater than the typical decay time of the glass ($\tau_p \sim 5$ μs). The experimental count mean and variance are 85.89 and 429.58, respectively, indicating the non-Poisson nature of this light. The solid curve represents the Neyman Type-A theoretical counting distribution, with the experimental values of count mean and variance ($\eta'\alpha'=4.0$), which provides an excellent fit to the data. The Poisson distribution with mean 85.89 (indicated by arrow) is shown as the dashed curve; clearly it bears no relation to the data.

In Fig. 2, the solid dots represent the observed normalized forward-recurrence-time probability density $\langle\tau\rangle P_1(\tau)$ (i.e., the time to the first cathodoluminescent photon arrival from an arbitrary starting time) measured by van Rijswijk (1976). The $YVO_4:Eu^{3+}$ phosphor was excited by a 10.2 keV electron beam. The solid curve is a plot of the theoretically expected result (Saleh and Teich, 1982a), which yields parameter values $\eta'\alpha'=9.6$ and $\tau'_p=0.5$ ms. The curved character of $\langle\tau\rangle P_1(\tau)$ on this semilogarithmic plot immediately indicates the non-Poisson nature of the photon emissions. It is well known that a Poisson process exhibits an exponential forward-recurrence-time probability

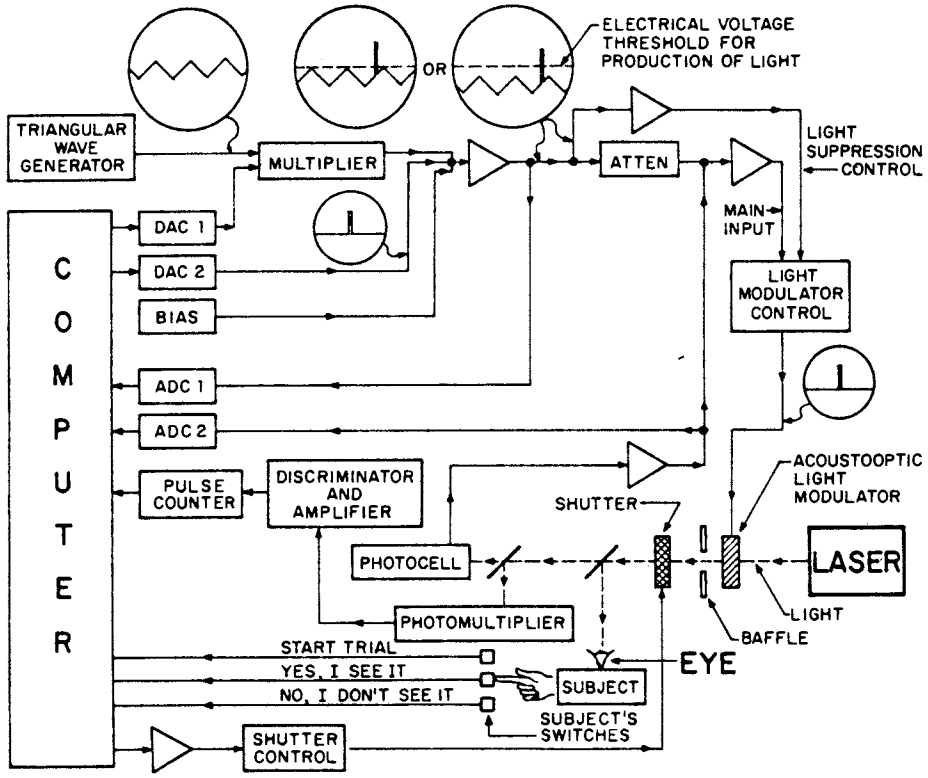

Fig. 3. Schematic representation of the experimental apparatus. The modulation scheme is illustrated in the upper portion of the figure. The optical arrangement is in the lower portion of the figure. (After Teich et al., 1982)

density function (Cox, 1962), yielding a straight line on such a plot.

The Neyman Type-A counting distribution is appropriate for stationary sources of light when $T' \gg \tau'_p$. It is also appropriate for nonstationary sources, such as a pulse of light, provided only that $\tau_s \ll \tau'_p + T$, where τ_s is the duration of the light pulse (Saleh and Teich, 1982b). Since $\tau'_p \simeq 0.5$ ms for light from a cathode-ray tube phosphor, and since the integration time of the eye $\gtrsim 50$ ms, the NTA is expected in both cases. For light from the $YVO_4:Eu^{3+}$ phosphor excited by 10.2 keV electrons, the counting distribution in the eye will be substantially broader than the Poisson.

3. Frequency of Seeing with Triangularly Modulated Poisson Light

3.1. Description of Experiments

We conducted a series of experiments identical to those reported in Part 1 (Teich et al., 1982) with the exception that the modulation depth M in these experiments was set equal to unity, rather than zero (see Fig. 3). Since the experimental procedure and results were previously reported in detail, only the essentials are repeated here.

The subject viewed a small dim red fixation target produced by a Maxwellian system and received a 5′ disk-shaped plane-polarized light stimulus in the left eye at $17\frac{1}{2}°$ horizontal eccentricity on the temporal retina. The stimulus was generated by a feedback-stabilized Spectra-Physics Model 162 Ar^+ ion laser that oscillated at 514.5 nm. The flash energy was controlled by an acousto-optic light modulator and the light was attenuated by neutral-density filters. An electronic shutter was opened just before, and closed just after, the presentation of the stimulus, to minimize the transmission of stray light to the subject. Three subject's switches were used to START the trial, and to indicate YES and NO responses. Absolute photometric calibrations were made using an EG&G radiometer with a silicon photodiode at the front end, substituted in place of the subject's eye.

Subjects were four males ranging in age from 23 to 38 years. All had normal vision. Alignment in the apparatus was maintained by the use of a dental-impression mouthbite. A trial consisted of the presentation of a 1-ms flash of light or of a blank. The occurrence of the 1-ms pulse was randomized with respect to the phase of the slow triangular wave (see Fig. 3); this led to a set of light intensities that were uniformly distributed over a specified range. The average flash energy was chosen quasi-randomly from one of 10 mean levels of the triangularly modulated light, separated by 0.115 log units; this yielded a total range of about 1 log unit. A block of trials consisted of 5

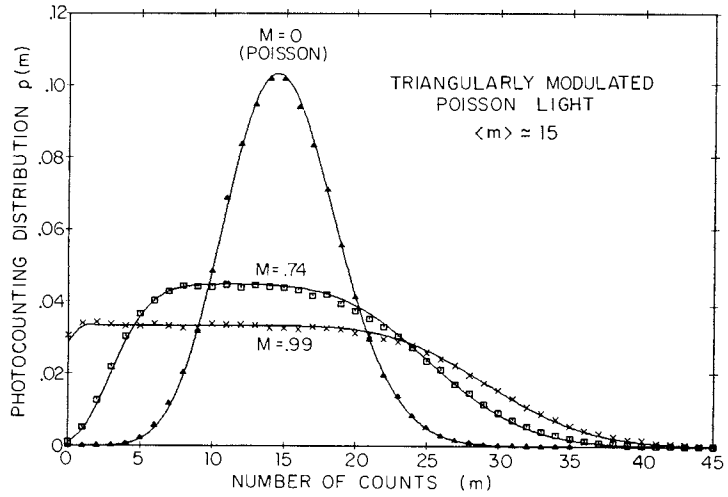

Fig. 4. Theoretical (solid curve) and experimental (data points) photocounting distributions [$p(m)$ vs m] registered by the photomultiplier tube for triangularly modulated Poisson light. The modulation depth M takes on three values: $M=0$ (▲), $M=0.74$ (□), and $M=0.99$ (×). The mean count is approximately the same for all three distributions ($\langle m\rangle \simeq 15$). The Poisson distribution results for $M=0$, whereas the flattest counting distribution is obtained for $M=1$. (After Teich and Vannucci, 1978)

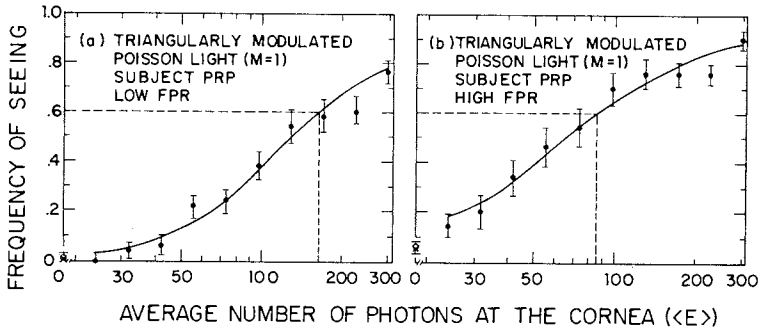

Fig. 5a and b. Frequency-of-seeing data (solid dots) generated by subject PRP with a triangularly modulated Poisson light stimulus (unity modulation depth and uniform phase) under low false-positive-rate conditions **a**, and high false-positive-rate conditions **b**. The left-most open circle represents the experimental false-positive rate $\hat{P}_F$ and the vertical bars are the ± 1-σ brackets. The solid curves and crosses (×) are derived from the simplified theoretical model discussed in the text

trials at each mean energy level plus 10 blanks, for a total of 60 trials per block. A session began with 35 min of dark adaptation, interrupted only by 2–4 blocks of preliminary experimental trials with $M=0$, to allow the subject to re-acquaint with the task. An experimental session was typically comprised of 6 blocks of trials and lasted from 1 to 1.5 h. A preliminary report of our experimental results was presented in abstract form (Teich et al., 1979).

3.2. *Experimental Photocounting Distribution*

The experimental photocounting distributions [$p(m)$ vs. m] registered by the photomultiplier tube (see Fig. 3) in the absence, and in the presence, of triangular modulation are presented in Fig. 4. These provide us with a measure of the distribution of photons sent to the subject. The data were gathered with a modulation period $T_M=1$ s and with a sampling time $T'=1$ ms. There were $N=2\times 10^5$ observation samples. The solid triangles (▲) represent data for $M=0$ (unmodulated light), the open squares (□) represent data for an intermediate modulation depth ($M=0.74$), and the crosses (×) represent data for nearly unity modulation depth ($M=0.99$). The mean number of counts for the three distributions is approximately the same ($\langle m\rangle \simeq 15$). It is evident that the theoretically calculated results represented by the solid curves (Teich and Diament, 1969, 1970) are in excellent agreement with the experimentally observed photocounting distributions for the three values of modulation depth employed (see Teich and Vannucci, 1978, for a complete discussion of these experiments). As anticipated, the unmodulated light ($M=0$) generated the Poisson photon-counting distribution (used for the experiments reported in Parts 1 and 2), whereas the triangularly modulated light with uniform sampling and nearly unity modulation depth (and with $T'\ll T_M$) produced the flattest photon-counting distribution.

3.3. *Frequency-of-Seeing Curves*

Frequency-of-seeing data were collected from the same four subjects as in Part 1, where Poisson light was used. The experimental frequency-of-seeing curves generated by subject PRP for unity modulation depth ($M\simeq 1$) are represented by the solid dots in Fig. 5a and b, for low- and high-false-positive rate (FPR) conditions, respectively. Again, the left-most open circle is the experimental false-positive rate $\hat{P}_F$ and the vertical bars surrounding each data point are the ± 1-σ brackets. The data exhibit very much the same behavior for all four subjects.

Comparing Fig. 5a with Fig. 2a of Part 1, and Fig. 5b with Fig. 3a of Part 1, it is apparent that the data obtained with modulated light are perceptibly shallower than those obtained with Poisson light; indeed, the highest values of the frequency of seeing lie well below unity. The physical reason for this is as follows. At any average energy level supplied to the cornea $\langle E\rangle$, the flat-counting distribution provides a greater number of trials with very low photon numbers than does the Poisson (see Fig. 4). A smaller fraction of these flashes are therefore detectable and this results in a decreased frequency of seeing. It is also important to note that, at this same average energy, some of the flashes will have energies up to a factor of 2 greater than with Poisson light (see Fig. 4). The subject is therefore physically exposed to flashes with greater numbers of photons, in an experiment using modulation. The only other physical distinction experienced by a subject in such an experiment is the greater randomization of flash energies. This arises because the variance of the flat-counting distribution for any level $\langle E\rangle$ is greater than that of the Poisson distribution (at the same level E), so that the number of photons delivered in that flash is more uncertain.

Considering, for the moment, the solid curves in Fig. 5 as empirical fits to the frequency-of-seeing data for triangularly modulated light, their shallowness relative to those for Poisson light means that the average number of photons at the cornea for 60% frequency of seeing is increased. Thus sensitivity and modulation depth are traded against other. Subject PRP, for example, required 162 photons with $M=1$ triangularly modulated Poisson light (see Fig. 5a) but only 147 photons with Poisson light (see Fig. 2a of Part 1). The FPRs are identical in the two cases (1.0%). The statistical character of the light, therefore, is a variable that must be considered in the list of conditions for optimal seeing. Comparing Fig. 5a and b, we see that there is also a substantial tradeoff between sensitivity and reliability, as observed in Part 1 for Poisson light.

3.4. Theory

In the context of the model presented in Part 1, the theoretical probability-of-detection curves are obtainable directly from our previous development. For all trials of fixed average energy $\langle E\rangle$, corresponding to a given point along the abscissa in Fig. 5, the light modulator (see upper portion of Fig. 3) provides different light-intensity (energy) values on each trial. These are drawn randomly, in accordance with a specified probability density function $P(E)$ with mean $\langle E\rangle$. Thus, the Poisson process (PP) generated by the laser is converted into a mixed or doubly stochastic Poisson process (DSPP) at the output of the modulator. For the modulation format at hand, $P(E)$ is uniformly distributed over a range of values specified by the modulation depth, and this leads to the family of flat-counting distributions (see Fig. 4).

Absorption and scattering at the cornea, and in the ocular medium and rods, reduces the energy by the factor η (see upper path in Fig. 6). If we assume that the quantum efficiency η is constant over the range of energy values encountered, the number of photons m registered at the retina, in the time T, will also satisfy the flat counting distribution (Teich and Diament, 1969, 1970; Teich and Vannucci, 1978)

$$\begin{aligned} p(m) &= \int_0^\infty p(m|\eta E)P(\eta E)d(\eta E) \\ &= \frac{\exp[-\langle m\rangle(1-M)]}{2M\langle m\rangle}\sum_{i=0}^{m}\frac{[\langle m\rangle(1-M)]^i}{i!} \\ &\quad - \frac{\exp[-\langle m\rangle(1+M)]}{2M\langle m\rangle}\sum_{i=0}^{m}\frac{[\langle m\rangle(1+M)]^i}{i!}, \end{aligned} \tag{2}$$

with mean count

$$\langle m\rangle = \eta\langle E\rangle \tag{3}$$

and variance (Prucnal and Teich, 1979)

$$\langle(\Delta m)^2\rangle = \langle m\rangle + M^2\langle m\rangle^2/3. \tag{4}$$

Of course, the variance is always greater than the mean. For triangularly modulated Poisson light, Eq. (2) above replaces Eq. (1b) in Part 1.

By analogy with the development presented in Part 1, we will probably not go far astray in supposing that the stimulus-induced counting distributions, both at the retinal ganglion cell level and at the output of the central processing and counting center, will be doubly stochastic versions of the Neyman Type-A (DSNTA) (see upper path in Fig. 6). This distribution is mathematically generated by simply replacing $p(m|\eta E)$, which appears in the summation of Eq. (2) of Part 1, by $p(m)$ as set forth in Eq. (2) above. Most simply, then, we view the central counting signal distribution as arising from a flat-counting stimulus distribution $p(m)$, associated with the modulated laser light, driving an independent Poisson neural counting distribution $p(s|m)$, associated with retinal and central multiplicative noise. The properties and moments of this class of distributions have recently been considered by Teich (1981).

If the stimulus is multiplied-Poisson light, instead of triangularly modulated light, the appropriate stimulus distribution will itself be the Neyman Type-A. In that case, the stimulus count variance retains a proportionality to the count mean [see Eq. (1)], and the assumed signal distribution at the counting center results from a cascade of three Poisson processes, as considered by Matsuo et al. (1982).

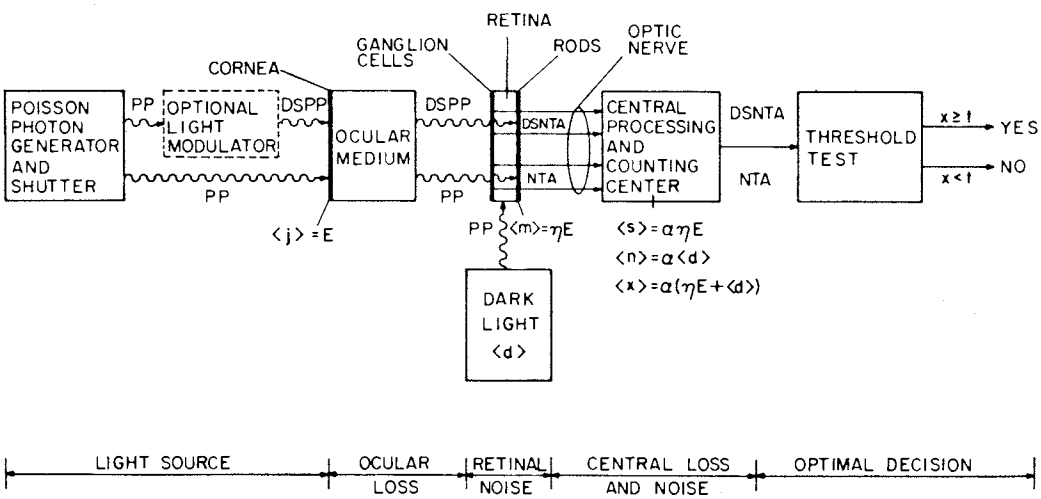

Fig. 6. Block diagram of model for visual system processing at threshold. The upper light path refers to DSPP light. (After Teich et al., 1982)

The characterizations described above will only be valid as long as the expanded energy excursions of the modulated light do not drive the statistical character of the underlying neural counting distribution away from its nominal form. If that occurs, the marginal probability obtained in the fashion described above would not be correct.

The noise distribution at the central processing and counting center is not subject to the light modulation, and clearly remains Neyman Type-A by the arguments presented previously. We are now in a position to generate our theoretical curves. We calculate the signal-plus-noise distribution, the false-positive probability, and the probability of detection from Eqs. (4), (5), and (6) of Part 1, respectively. The mathematics is not quite as tidy as it was in the case of Poisson light, and the computer calculations required for the various curves can become tedious. The asymptotic normality of the Neyman Type-A distribution (Teich, 1981) might be useful in some cases. But we've set it all down very directly, and it can be done.

3.5. Discussion

Instead, we choose to approach the problem from a rather different point of view. We break it into small and separable pieces, examine their interrelationships and then synthesize them, hoping to learn something about the relative importance of various mechanisms associated with threshold vision along the way. We begin by noting a special property of the modulated light that will enable us to make some drastic simplifications that will be instructive; it is the large excess variance introduced by the energy fluctuations of the stimulus. For reasonable values of the average number of absorbed photons at the retina (say $\langle m \rangle \gtrsim 6$), and unity modulation depth ($M = 1$), the second term on the right-hand side of Eq. (4) dominates the first term, which represents the irreducible Poisson fluctuations of the light. A similar expression exists for the DSNTA variance [Teich, 1981, Eq. (25b)] and it turns out that for $\alpha = 1/2$, the multiplicative noise (Neyman) fluctuations are also negligible in this regime. If we ignore both the irreducible Poisson and multiplicative fluctuations then, and also forget about additive noise, we end up with a set of theoretical probability-of-detection curves derived from summated uniform distributions (since E is uniformly distributed). Plotted out, these look pretty much like ordinary psychometric functions except that their rise above zero at a specified value of $\langle E \rangle$ has a discontinuous first derivative. We understand this to be because of the sharp edge of the uniform $P(E)$ distribution. The same approximation for Poisson light doesn't appear to make any sense, at first blush, because $P(E)$ is a Dirac delta function which produces step psychometric functions. We shall return to this point in Sect. 4.

With very little additional work, we can be a bit more sophisticated, and explore an interesting connection. Since the magnitude of the Neyman fluctuations is just about half that of the Poisson fluctuations (for $\alpha = 1/2$), a slightly better approximation can be constructed by including the stimulus-energy and irreducible Poisson fluctuations, still ignoring the multiplicative and additive noise. The theoretical probability-of-detection curves are then derived from summated flat-counting distributions (see Fig. 4). These strongly resemble the set derived from the uniform distributions, but they rise gradually with a continuous first derivative. For high modulation depths M, both of these families of curves are substantially shallower than the summated Poissons that we are used to seeing. The same approximation for Poisson light contains no contribution from stimulus energy fluctuations, since there are none, so the

psychometric functions are simply derived from summated Poisson distributions.

This is, of course, precisely the model used by HSP in connection with their Poisson light experiments reported in 1942, and so we decided to examine this approximation for both modulated and Poisson light in one of our early studies (Matin et al., 1978). The mean energy of the modulated light was maintained equal to the energy of the unmodulated light ($\langle E\rangle = E$) for all values of E. It turned out that we were able to provide quite good theoretical fits to low-FPR frequency-of-seeing data for all 3 modulation depths employed ($M=0$, $M=1/\sqrt{2}$, and $M=1$), simultaneously, with a fixed value of the threshold count t for each subject. (Curves for the different modulation depths are distinguished by their different shapes and slopes.) The values of t extracted from the data for our four subjects fell between 4 and 6, and a photometric measurement of the light energy at the cornea allowed us to infer a psychophysical quantum efficiency $\eta \simeq 5\%$ (Matin et al., 1978). Of course the theory predicted zero falsereport probability.

The experimental results are such, that it appears we are getting the same information from the data without modulation and with modulation, i.e., both sets fit well; t and η are the same. (A minor point is that the data with modulation are, and should be, somewhat more erratic because the frequency of seeing increases more slowly and the data samples therefore have larger standard deviations.) It would be erroneous to conclude, however, that the agreement of these probability-of-detection curves with the data for different values of M provides independent justification for an HSP-type model in which stimulus fluctuations are the dominant source of variability. Indeed it does not. As indicated in Sect. 3.3, the two physical distinctions experienced by a subject undergoing an experiment with different values of M are: (1) a greater randomization of the light intensities for experiments conducted with large M and (2) a greater range of flash energies for experiments conducted with large M (up to a factor of 2 for $M=1$; see Fig. 4). The only conclusion that we may draw is that neither of these two factors produces a resolvable deviation of this theory with experiment, and therefore that experiments with modulated light do not provide additional information about threshold visual mechanisms here. Indeed, the usual shortcomings associated with a model at this level of approximation appear for all values of M: (1) the inability to account for nonzero false-positive rates and (2) a psychophysical value for η that is inconsistent with the photometric value.

The next step may come as no surprise to the reader. We include Poisson additive dark noise with our stimulus-energy and Poisson-photon fluctuations, leaving aside only the multiplicative noise. This is a convenient step for us. In the first place, it permits a false-positive probability to be incorporated into our mathematical structure in a straightforward manner, and in the second place, all of the theoretical calculations have already been carried out in connection with another study (Teich and Cantor, 1978). Furthermore, this is analogous to the model used by Barlow (1956) for Poisson light (in which case the stimulus energy is constant) so that it affords us an opportunity to examine the role of stimulus energy fluctuations at this level of approximation.

The solid curves and crosses ($\times$) in Fig. 5 represent the results of a 3-parameter fit of the theoretical probability-of-detection curves, discussed in the previous paragraph, to the frequency-of-seeing data. The procedure was designed to minimize the sum of squares. The model parameters associated with the best-fitting curves in Fig. 5a and b are $\{\eta=3.9\%, \langle n\rangle=2.7, t=8\}$ and $\{\eta=8\%, \langle n\rangle=8.6, t=14\}$, respectively. Because of the complexity involved in dealing with all of the parameters, we did not attempt to simultaneously fit data for different values of M; (we also collected data for $M=1/\sqrt{2}$, and for sinusoidally modulated light with $M=1$.)

The fits turn out to be excellent for all subjects, providing yet another illustration of the many ways in which virtually identical probability-of-detection curves can be generated. But, just as for the case of Poisson light discussed in Part 1, the model parameters jump about unpredictably from data set to data set, showing no particular pattern. The associated theoretical false-positive probabilities also appear to be smaller than the measured FPRs, and it may be that the use of Poisson noise again causes difficulties. It therefore seems that here, too, the modulated data provide us with no new information regarding threshold mechanisms and should not be considered as in any way validating this model.

We could, of course, proceed yet another step and incorporate the multiplicative noise to account for the statistical behavior of the ganglion cell, and for central loss and noise, in the manner described in Sect. 3.4. That would bring us full circle. Indeed we have little doubt that this is a proper theory, and will provide very good agreement with the data because of what we have already learned; the expanded energy excursions associated with the modulated light appear to leave the statistical character of the underlying neural counting distribution intact, within the resolution of our experiments. We therefore avoid the complications associated with extracting model parameters from the modulated-light data. But we point out, as is clear from our earlier discussion, that the sensitivity-reliability curve presented in Fig. 6 of Part 1 is specific

to Poisson light. The appropriate curve for DSPP light of arbitrary statistical character can be constructed by the methods outlined above.

We conclude that an HSP-type experiment, conducted with bunched light, such as triangularly modulated light or multiplied-Poisson light, generates psychometric functions that differ in shape from those observed with Poisson light (they are not as steep). The use of such light sources should therefore be avoided when conducting threshold experiments, since the excess fluctuations tend to obscure the visual mechanisms of interest. In the next section, we discuss the prospects for using antibunched light, in our attempts to unravel the operation of the visual system at low light levels.

4. Theoretical Probability-of-Detection Curves with Antibunched Light

Frequency-of-seeing experiments carried out with antibunched light can, in principle, provide a great deal of information about the operation of the visual system near threshold. Unfortunately, sources emitting fixed numbers of quanta in a given time interval are not yet available as black boxes that can be plugged into the nearest wall outlet, and there are problems relating to the absorption of such radiation that we will deal with at the end of this section. There is an extensive current research effort in quantum optics to develop sources with at least some antibunched ($R<1$) behavior (Glauber, 1963a, b; Peřina, 1972; Stoler, 1974; Kimble et al., 1977; Mandel, 1979). In the following we consider, from a theoretical point of view, some of the consequences of using antibunched light in frequency-of-seeing experiments.

The ideal antibunched source emits a constant number of photons $\langle j\rangle$, in the time interval T', so that the counting distribution is given by the Dirac delta function

$$p(j)=\delta(j-\langle j\rangle), \tag{5}$$

with mean count $\langle j\rangle$ and variance $\langle(\Delta j)^2\rangle=0$. This is the so-called Fock or number state (Peřina, 1972). For the moment, let us assume that these photons are delivered directly to the retina, and that the number of photons absorbed by the rods also obeys this distribution, so that

$$p(m)=\delta(m-\langle m\rangle) \tag{6}$$

with mean count $\langle m\rangle$ and variance $\langle(\Delta m)^2\rangle=0$. We shall return to this point later. It is now routine to calculate the behavior of any particular model of threshold visual detection by simply letting Eq. (6) replace Eq. (1b) in Part 1 [much as we let Eq. (2) replace Eq. (1b) in Part 1, for the bunched light considered earlier]. Because of the mathematical properties of the Dirac delta function, this is a very simple enterprise, and so we will run through the heirarchy of models considered previously.

By definition, there are neither stimulus-energy nor Poisson fluctuations in this case. A moment's thought, and our previous discussion, tells us that the HSP model with such perfectly antibunched rod excitations leads to step psychometric functions. The threshold t is exactly determined by the value $\langle m\rangle$ at which the step occurs, and there is nothing more to be known.

If we now include additive independent dark light, of arbitrary statistical properties, $p_N(n|\langle d\rangle)$, the signal-plus-noise distribution $p_{SN}(x|\langle d\rangle,\langle m\rangle)$ is, of course, the convolution of the noise distribution with a delta-function signal distribution. This signal-plus-noise distribution then exhibits precisely the same shape as the noise distribution alone, but translates by integer increments along the abscissa x as the rod excitation number (and therefore, by assumption, the signal photon number) increases. Psychometric functions plotted on an abscissa linear in $\langle m\rangle$ will, in this case, maintain a constant shape regardless of the threshold. For a threshold value greater than the maximum noise count (in which case the false-positive probability will be zero), that shape will be precisely the mirror image of the integral of the noise distribution, so that the form of the noise probability distribution itself is exactly recoverable. Furthermore, since P_F and P_D are measurable for each value of $\langle m\rangle$, the mean of the noise distribution $\langle n\rangle$ and the threshold t can also be determined. In the context of this model, then, number-state rod excitations provide the ultimate tool in extracting all of the characteristics of the visual system at threshold.

Finally, we consider what happens when multiplicative noise is included. This, of course, is the model presented in Fig. 6, but now the rod excitations are described neither by Poisson nor by doubly stochastic Poisson distributions, but rather by the delta-function distribution presented in Eq. (6). Replacing $p(m|\eta E)$ in the summation of Eq. (2) in Part 1, by $p(m)$, as given in Eq. (6), we see immediately that the central-counting signal distribution is

$$p(s|\langle m\rangle)=\sum_{m=0}^{\infty}p(s|m)\delta(m-\langle m\rangle)=\frac{(\alpha\langle m\rangle)^s e^{-\alpha\langle m\rangle}}{s!}. \tag{7}$$

This is a simple Poisson distribution with mean $\langle s\rangle=\alpha\langle m\rangle$.

The outcome is understood most simply as follows. There are neither stimulus-energy nor Poisson photon fluctuations, so that the fixed number of rods excited on every trial ($\alpha\langle m\rangle$) drives an independent Poisson neural counting distribution associated with retinal and central processing. The noise distribution at the

central processing and counting center is unaffected by the presence, or absence, of the signal so it remains Neyman Type-A. The result is a signal-plus-noise distribution that is the convolution of a Poisson and a Neyman Type-A, with parameters α, $\langle d \rangle$, and t. The false-positive probability is calculated from Eq. (5) of Part 1, and the probability of detection from Eq. (6) of Part 1. The outcome in this case is no simpler to calculate than when Poisson light is delivered to the retina. However, since the psychometric functions will change shape for different values of the threshold, the three models discussed in this section may be experimentally distinguishable. Of course, similar calculations could be carried out with any model we choose to investigate.

The alert reader will have noted that we have not yet introduced the quantum efficiency η into our discussion. We have assumed to this point, rather, that the number distribution of excited rods could be precisely controlled [Eq. (6)]. The reason for this is straightforward: Unlike its effect on the DSPP, an absorption medium will substantially alter the statistical properties of antibunched light. This can be most easily visualized in terms of random deletions from a deterministic pulse train, which convert it into a process with a binomial distribution, whose value of R will be closer to, but still below, unity (Teich and Saleh, 1982). Thus, the ocular medium, and the imperfect absorption by the rods, become crucial factors in this case. We would therefore expect that in an ordinary frequency-of-seeing experiment, it will be difficult to direct antibunched light through the ocular medium and retina, and still have it produce substantially antibunched rod excitations. Nevertheless, it is certainly reasonable to believe that the future will bring more than one cleverly designed experiment, perhaps using yet-to-be-developed fiber-quantum-optic techniques, that will permit the use of antibunched light to probe the workings of the visual system near threshold.

References

Barlow, H.B.: Retinal noise and absolute threshold. J. Opt. Soc. Am. **46**, 634–639 (1956)

Cox, D.R.: Renewal theory. London: Methuen 1962

Glauber, R.J.: The quantum theory of optical coherence. Phys. Rev. **130**, 2529–2539 (1963a)

Glauber, R.J.: Coherent and incoherent states of the radiation field. Phys. Rev. **131**, 2766–2788 (1963b)

Hecht, S., Shlaer, S., Pirenne, M.H.: Energy, quanta, and vision. J. Gen. Physiol. **25**, 819–840 (1942)

Kimble, H.J., Dagenais, M., Mandel, L.: Photon antibunching in resonance fluorescence. Phys. Rev. Lett. **39**, 691–695 (1977)

Mandel, L.: Sub-Poissonian photon statistics in resonance fluorescence. Opt. Lett. **4**, 205–207 (1979)

Matin, L., Teich, M.C., Breton, M.E., Vannucci, G., Prucnal, P.R., McGill, W.J.: Quantum requirements at the absolute threshold with non-Poisson visual stimuli (abstract). Invest. Ophthal. Vis. Sci. (ARVO supplement) **17**, 132–133 (1978)

Matsuo, K., Saleh, B.E.A., Teich, M.C.: Cascaded Poisson processes (submitted for publication) (1982)

Neyman, J.: On a new class of "contagious" distributions, applicable in entomology and bacteriology. Ann. Math. Stat. **10**, 35–57 (1939)

Peřina, J.: Coherence of light. London: Van Nostrand-Reinhold 1972

Prucnal, P.R., Teich, M.C.: Statistical properties of counting distributions for intensity-modulated sources. J. Opt. Soc. Am. **69**, 539–544 (1979)

Prucnal, P.R., Teich, M.C.: Multiplication noise in the human visual system at threshold: 2. Probit estimation of parameters. Biol. Cybern. **43**, 87–96 (1982)

Saleh, B.E.A., Teich, M.C.: Multiplied-Poisson noise in pulse, particle, and photon detection. Proc. IEEE **70**, 229–245 (1982a)

Saleh, B.E.A., Teich, M.C.: Statistical properties of a nonstationary Neyman-Scott cluster process (submitted for publication) (1982b)

Stoler, D.: Photon antibunching and possible ways to observe it. Phys. Rev. Lett. **33**, 1397–1400 (1974)

Teich, M.C.: Role of the doubly stochastic Neyman type-A and Thomas counting distributions in photon detection. Appl. Opt. **20**, 2457–2467 (1981)

Teich, M.C., Cantor, B.I.: Information, error, and imaging in deadtime-perturbed doubly stochastic Poisson counting systems. IEEE J. Quant. Electron. QE-**14**, 993–1003 (1978)

Teich, M.C., Diament, P.: Flat counting distribution for triangularly-modulated Poisson process. Phys. Lett. **30** A, 93–94 (1969)

Teich, M.C., Diament, P.: Observation of flat counting distribution for Poisson process with linearly-swept mean. J. Appl. Phys. **41**, 415–416 (1970)

Teich, M.C., Saleh, B.E.A.: Fluctuation properties of multiplied-Poisson light: measurement of the photon-counting distribution for radioluminescence radiation from glass. Phys. Rev. A**24**, 1651–1654 (1981a)

Teich, M.C., Saleh, B.E.A.: Interevent-time statistics for shot-noise-driven self-exciting point processes in photon detection. J. Opt. Soc. Am. **71**, 771–776 (1981b)

Teich, M.C., Saleh, B.E.A.: The effects of random deletion and additive noise on bunched and antibunched photon-counting statistics. Opt. Lett. 7 (in press) (1982)

Teich, M.C., Vannucci, G.: Observation of dead-time-modified photocounting distributions for modulated laser radiation. J. Opt. Soc. Am. **68**, 1338–1342 (1978)

Teich, M.C., Prucnal, P.R., Vannucci, G., Breton, M.E., McGill, W.J.: Role of quantum fluctuations and the Neyman type-A distribution in human vision (abstract). J. Opt. Soc. Am. **69**, 1469 (1979)

Teich, M.C., Prucnal, P.R., Vannucci, G., Breton, M.E., McGill, W.J.: Multiplication noise in the human visual system at threshold: 1. Quantum fluctuations and minimum detectable energy. J. Opt. Soc. Am. **72**, 419–431 (1982)

van Meeteren, A.: On the detective quantum efficiency of the human eye. Vision Res. **18**, 257–267 (1978)

van Rijswijk, F.C.: Photon statistics of characteristic cathodoluminescence radiation. II. Experiment. Physica **82**B, 205–215 (1976)

Received: October 29, 1981

Prof. Dr. Malvin Carl Teich
Columbia University
Department of Electrical Engineering
Seeley W. Mudd Building
New York, NY 10027
USA